Open access • Journal Article • DOI:10.1029/JA080I004P00595

The motion of a proton in the equatorial magnetosphere — Source link

David P. Stern

Institutions: Goddard Space Flight Center

Published on: 01 Feb 1975 - Journal of Geophysical Research (John Wiley & Sons, Ltd)

Topics: Ring current, Magnetosphere, Magnetic dipole, Electric field and Magnetosphere particle motion

2N64

X-602-74-160
PREPRINT

NASA TM X- 70667

THE MOTION OF A PROTON IN THE EQUATORIAL MAGNETOSPHERE

DAVID STERN

MAY 1974

GSFC — GODDARD SPACE FLIGHT CENTER —
GREENBELT, MARYLAND

For information concerning availability
of this document contact:

Technical Information Division, Code 250
Goddard Space Flight Center
Greenbelt, Maryland 20771

(Telephone 301-982-4488)

The Motion of a Proton in the Equatorial Magnetosphere

David P. Stern
Theoretical Studies Branch
Goddard Space Flight Center
Greenbelt, Maryland 20771

Introduction

A proton of low energy moving in the equatorial plane of the earth will experience drift motions due to both the magnetic field (magnetic gradient drift only, if the field is assumed to be that of a dipole) and the electric field. The electric drift again separates into two parts - the drift due to the "main" electric field (or "convection electric field") existing in the frame of the earth, and that due to the earth's rotation.

Such motion has been analyzed by Chen [1970] who assumed that the main field in the equatorial plane is a constant field from dawn to dusk. He obtained a somewhat complex variety of proton orbits: the main purpose of this work is to classify such orbits and to devise a simple procedure by which one can determine, in the energy spectrum observed by a satellite in the equator, which energies (of equatorial particles) correspond to trapped trajectories and which to open ones. The electric field used here [Stern, 1974] differs somewhat from the model used by Chen, giving a more realistic fit to high-latitude observations of the electric field, but all results obtained here could be easily generalized for Chen's model.

One result indicated by this work is that at distances of 4 - 6 earth radii, a transition from trapped proton orbits to open trajectories leading to the tail occurs at about 10 kev, the precise value depending upon local time. Such a transition also seems to be indicated by particle observations of Smith and Hoffman [1973a, b], using Explorer 45. The energy spectrum (at magnetically quiet times) of equatorial protons above this energy can be explained by charge exchange [Smith and Hoffman, 1974], but increased flux observed below it seems to be related to the influx of particles on open orbits from the tail.

Qualitatively the situation may be viewed as follows. At very low energies and near enough to earth, electric drift due to the co-rotation field is dominant, and charged particles tend to co-rotate and are thus trapped.

At relatively high energies all electric drifts may be neglected and guiding center motion is mainly due to magnetic drift, which also tends to keep particles trapped in the vicinity of the earth.

Now for equatorial electrons these two drifts are in the same direction and tend to reinforce each other, while for equatorial protons the directions are opposed. There may thus exist for protons an intermediate energy range in which these two drifts approximately cancel and the drift in the main electric field ("convection field") dominates the motion: drift orbits due to this field are open and generally follow the noon-midnight direction, allowing an explanation for the previously mentioned features of the energy spectrum.

The Electric Field

Following previous work [Stern, 1974] we assume that the main electric field in the rotating frame has a form derivable from a scalar potential. On closed field lines our model gives

$$\underline{E} = - \nabla \phi_1 \qquad (1)$$

$$\phi_1 = - \phi_0 \left(\alpha_0 / \alpha \right)^{k/2} \sin \varphi \qquad (2)$$

Here α is an Euler potential for the dipole magnetic field (which is the magnetic configuration assumed), given by

$$\alpha = a g_1^0 \rho^{-1} \sin^2 \theta \qquad (3)$$

where $g_1^0 \cong - 3.1 \cdot 10^{-5}$ MKS is the dipole term in the harmonic expansion of the earth's magnetic field, a is the earth's radius and $\rho = r/a$. Also, α_0 is the value of α on the boundary of the polar cap and $2 \phi_0$ is assumed to be the voltage across the cap. The power k reflects the rate with which $|\underline{E}|$ decreases near the polar cap boundary: Chen's model is obtained if $k = 2$, but electric field measurements at high latitudes [Heppner, 1972] suggest that $k = 4$ is more realistic, and this value will be assumed here.

The total electric field - with axisymmetric rotation added - is

$$\underline{E} = - \nabla (\phi_1 + \phi_2) \qquad (4)$$

with $$\phi_2 = a \omega \alpha \qquad (5)$$

where $\omega \cong 7.3 \cdot 10^{-5}$ rad/sec is the earth's angular velocity. Thus in the equatorial plane, with $k = 4$

$$\phi = - \phi_0 (\alpha_0 / a\, g_1^0)^2 \rho^2 \sin \varphi + a^2 g_1^0 \omega / \rho \qquad (6)$$

The Hamiltonian

The Hamiltonian for the motion of a particle of charge e in the dipole equator, in the presence of the fields described here, is

$$H = \mu B + e \phi \qquad (7)$$

In dealing with protons, if e is dropped and ϕ is reckoned in volts, then all energies are in electron volts and the magnetic moment μ of the particle (which is assumed to be conserved) is conveniently expressed in ev/B . The magnetic field B itself is given by

$$B = |g_1^0| / \rho^3 \qquad (8)$$

The Hamiltonian is a constant of the motion - that is, contours of constant H in the (ρ, φ) plane for any given μ describe trajectories of protons having that value of μ .

For convenience we may use the constancy of $H' = H / |g_1^0|$, which can be expressed in terms of positive constants q and p (no relation to canonical variables)

$$H' = \mu \rho^{-3} - q \rho^2 \sin\varphi - p \rho^{-1} \qquad (9)$$

where

$$q = - \phi_o (\alpha_o / a\, g_1^o)^2 \, / |g_1^o| \qquad (10)$$

$$p = a^2 \omega \cong 2.9 \cdot 10^9 \ m^2/sec \qquad (11)$$

If the radius of the polar cap is taken as $a/4$ and the mean electric field there is E_o volts/m , then

$$q \cong 2 \cdot 10^8 \ E_o \qquad (12)$$

The calculation may be made more general if as many constants as possible are removed by suitable normalization of quantities. To remove q and p , one first divides (9) by q and then defines new units of length, such that ρ is replaced by

$$R = \rho \, (q/p)^{1/3} \qquad (13)$$

Specifically, if one defines

$$W = H'/(q\, p^2)^{1/3} \qquad (14)$$

$$M = \mu \, (q^2/p^5)^{1/3} \qquad (15)$$

then equation (9) transforms into

$$W = M R^{-3} - R^2 \sin\varphi - R^{-1} \qquad (16)$$

which will be the basic conservation law used in what follows.

Qualitative Analysis

If W is considered as a function of (R, φ), proton trajectories in the equatorial plane will be given by contours of constant W and "last closed trajectories" will be characterized by contours which cross themselves (see Figures 1, 2 and 3). At a crossing point the direction of ∇W is not defined and therefore

$$\nabla W = 0 \qquad (17)$$

The reverse however is not true : ∇W may vanish at a point which is not a crossing point but rather the limit point of a set of nested closed trajectories (e.g. point P_2 in Figures 1 and 2).

The φ-derivative of (16) shows that (17) may only be satisfied on the dawn-dusk line, at points where

$$\sin \varphi = \pm 1 \qquad (18)$$

It is instructive to examine the dawn side and the dusk side of that line separately.

On the dusk side ($\sin \varphi = 1$) the vanishing of the R-derivative of (16) gives

$$1 = 3 M R^{-2} + 2 R^3 = \xi(R) \qquad (19)$$

The function $\xi(R)$ tends to infinity at both 0 and ∞ and it has a single minimum at $R = M^{1/5}$. The value of $\xi(R)$ at the minimum point will be smaller or larger than 1, depending on whether M is less or more than

$$M_o = 5^{-5/3} \cong 0.0684 \qquad (20)$$

and accordingly (19) - and hence (17) - will be satisfied either at two points or at no points at all.

On the dawn side (17) requires

$$1 = 3 M R^{-2} - 2 R^{3} = \eta(R) \qquad (21)$$

The function $\eta(R)$ has a negative derivative and descends continuously from $\eta(0) = \infty$ to $\eta(\infty) = -\infty$. There exists therefore on the dawn side a single solution of (17) for all values of M .

The values of W corresponding to solutions of (17) will be called critical values. In particular, W_1 and W_2 will denote critical values corresponding to the dusk side (W_1 having a larger value of R than W_2) and W_3 will denote critical values on the dawn side. In all cases the critical values depend on M , so that W_1, W_2 and W_3 are all functions of M , displayed in graphical form in Figure 4 .

Interpretation

If the point for which W_i was derived is a crossing point, then the contour $W(M, R, \varphi) = W_i(M)$, for any given M, gives in part the boundary between a region of trapped trajectories and a region of "open" ones. If, on the other hand, W_i represents a limit point of a nested set of trapped trajectories, then the line $W(M,R,\varphi) = W_i(M)$ shrinks to a point and does not properly exist. It will turn out that the first case applies to W_1 and W_3 while the second holds for W_2 .

As M is varied, the map of contours of constant $W(M, R, \varphi)$ gradually changes. Three regimes then exist and will be denoted by numbers 1, 2 and 3 ; they are illustrated by the Figures bearing the same numbers and by the numbered ranges of M in Figure 4 . In regime 1 (illustrated schematically by Figure 1 and also by Figures 2 in the work of Chen [1970]) $W_1 > W_3$ and the trapped region defined by W_1 encloses the one which is defined by W_3, so that it alone determines whether an orbit is trapped or not. In regime 2 (Figure 2 ; also Figures 3b and 4a in the work of Chen [1970] , where Figure 3a gives the transition between regimes 1 and 2) $W_1 < W_3$ and the trapped regions determined by W_1 and W_3 are disjoint. Finally, in regime 3 (Figure 3 here, and Figures 4b and 5 in Chen's work) the trapped

region defined by W_1 disappears, since (19) no longer has any real solutions, leaving just the trapped region defined by W_3, which in all three regions surrounds the origin.

It is instructive to sketch qualitatively the variation of W along the dawn-dusk line, and this is done in the lower parts of Figures 1, 2 and 3 . Note that this variation has extrema at all points at which (17) holds, although the shapes of these extrema are only schematically shown in the figures.

Each of the contours corresponding to a crossing point in one of these figures - except for the W_3 contour of Figure 1 - consists of two parts - one of them forming a closed loop, the other extending to infinity at both its ends. These will be called the closed and open branches of the contours of W_1 or W_3 .

It is easily shown that the crossing point - which belongs to both branches - is the point closest to the origin on the open branch and the point farthest from the origin on the closed one. The proof is as follows. For given fixed values of W_i and M , these contours satisfy the equation

$$W_i = M R^{-3} \mp R^2 \sin\varphi - R^{-1} \qquad (22)$$

(plus for $i = 3$, minus for $i = 1$). They therefore define a functional relationship $R = R(\varphi)$, with an inverse function $\varphi = \varphi(R)$. At the point on the contour at which R is extremal $dR/d\varphi$ vanishes and therefore $d\varphi/dR$ diverges. From (22), however,

$$\pm \cos\varphi \; d\varphi/dR = 2 W_i R^{-3} - 5 M R^{-6} + 3 R^{-4} \qquad (23)$$

Therefore such extremal points only occur in the dawn - dusk plane where $\cos\varphi$ vanishes. There exists only one such point on open branches, namely the crossing point, which therefore is a point of minimum R .

In the immediate vicinity of the crossing point the contours of constant W_i assume the form of an X , and the curve of constant R through that point is a circular arc tangential to a line which bisects that X . One side of the X then belongs to the open branch and R is minimal there, from which it follows that for the other side, belonging to the closed branch, R is maximal at the crossing point. However, the closed branches (except for that of W_3 in Figure 1) have only <u>two</u> points with $\cos\varphi = 0$. The other point with that property is therefore a minimum point for R , showing that R at the crossing point is an absolute maximum value for the entire closed branch.

The Profile Line

Suppose one is observing equatorial protons with various energies at some given point (r, φ) at which the magnetic field intensity is B . Given the various constants of the model one can then derive R for the observation point and values of M for each observed value of the kinetic energy K . If ρ is the distance in earth radii and μ is the magnetic moment in kev/gamma, then

$$R = 0.412\ E_o^{1/3}\ \rho \qquad (24)$$

$$M = 58.4\ E_o^{2/3}\ \mu \qquad (25)$$

The objective of this section is to develop in that case a simple way of distinguishing which values of M (or of K) correspond to open trajectories and which to closed ones trapped near the earth.

For every value of observed energy there corresponds by (25) a value of M , and by equation (16) the corresponding value of W can then be computed. Since (R, φ) are fixed, equation (16) shows that all related pairs of values (W, M) observed at the given point belong to a single straight line in the (W, M) plane, which will be called the <u>profile line</u> of the observation point. The type of trajectory may change from trapped to free or vice versa only at points at which the profile line crosses one of

the lines

$$W = W_1(M) \quad , \quad W = W_3(M) \tag{26}$$

To establish which crossings do represent a change in type of trajectory we follow the profile line from its right-hand side, corresponding to large values of M . Equation (21) shows that for any given M the normalized radial distance R_3 to the crossing point of W_3 satisfies

$$3\,M = R_3^2 + 2\,R_3^5 \tag{27}$$

In the limit of large R_3

$$\begin{aligned} M &= 2\,R_3^5/3 \\ W_3 &= 5\,R_3^2/3 \end{aligned} \tag{28}$$

On the dusk side the line $W = W_3$ then approaches the origin within a distance $R_3\delta$, where $\delta \leq 1$ (see Figure 3). Substituting in (16) gives, in the same limit

$$\begin{aligned} 2 - 3\,\delta^5 &= 5\,\delta^3 \\ &\leq 5\,\delta^{2.5} \end{aligned} \tag{29}$$

The inequality yields

$$\delta \geq 3^{-0.4} \tag{30}$$

meaning that the normalized <u>minimum</u> distance R on the closed branch of $W = W_3$ <u>also</u> becomes large under these circumstances. Since the value of R for the observation point is fixed and finite, it follows that the upper end $(M \to \infty)$ of the profile line <u>always</u> starts at points corresponding to the interior of the closed branch in Figure 3 .

At $M = 0$ equation (27) shows that $R_3 \to 0$, i.e. the observation point is outside the inner closed branch of W_3. Thus the profile line crosses the line $W = W_3(M)$ at least once. If the first crossing of this kind occurs in regimes 2 or 3, it changes the type of trajectory from trapped to open. If the change occurs in regime 1, no change occurs, because all crossings of W_3 there are from one trapped mode to another (see Figure 1).

A crossing of the line $W = W_1(M)$ will change the status of the trajectories only if the closed branch of that line is involved. This will generally be the case, but a simple check is at any rate available to ascertain this, based on the theorem proved in the preceding section. To perform this check, one notes the value of M associated with the crossing point and then compares the value of R associated with this value of M by equation (21) (Table 1 and Figure 5) with the value of R derived for the observation point. If the latter is smaller, the crossing is on the closed branch.

It is interesting to examine the family of profile lines having the same value R_o of the normalized radial distance but different values of magnetic longitude φ. All these lines are parallel and are located inside the strip bounded by

$$W = M R_o^{-3} - R_o^2 + R_o^{-1} \qquad (31)$$

and

$$W = M R_o^{-3} + R_o^2 + R_o^{-1} \qquad (32)$$

For $R = R_o$ there will exist some positive solution M_o for M satisfying equation (21). The point on the profile line (32) corresponding to M_o then also belongs to the line $W = W_3(M)$, since both conditions (16) and (21) are fulfilled. In fact, the profile line will be tangential to the W_3 curve, since (it can be shown) both lines have the same slope at M_o. Similarly, the bounding line (31) is tangential to $W = W_2(M)$, provided the two lines meet. The situation is illustrated in Figure 6, for a radial distance of 5 earth radii and given $E_o = 0.01$ volt/m. A third line in the middle of the strip represents observations on the noon-midnight meridian, and heavily drawn portions of the profile lines represent open trajectories.

Conclusions

At distances of the order of 5 earth radii, there will exist for each observation point a range of proton energies for which trajectories are connected to the tail, while at lower and higher energies trajectories are trapped.

Smith and Hoffman [1973a, Fig.3] observe at quiet times an energy spectrum of equatorial protons which has two peaks, separated by a dip in the range 10 - 100 kev. The dip and the high energy peak can be explained [Smith and Hoffman 1973b, 1974] in terms of charge exchange effects, but the peak at the lower energies falls in the region in which the present theory indicates open trajectories and therefore appears to represent particles entering from the tail, the source being intense enough to overcome charge-exchange losses.

The range of open trajectories is also expected to have a low-energy boundary and this can be compared to a similar boundary observed by McIlwain [1972, Figure 6], shifting towards lower energies as local time varies from evening to early morning hours.

This shift agrees with the predictions of the model, but there exist notable differences the most significant being the absence of a similar effect on the day side. However, plasma sheet particles require relatively long times to reach the day side, during which their motion may be modified, and in addition, a better model of the magnetic field is probably needed at 6.6 earth radii, where McIlwain's observations were made.

The actual electric field of the earth varies in time and therefore, strictly speaking, it cannot be represented by a scalar potential. If however its variation is slow and consists mainly of a change in E_o, then to lowest approximation the method may still be used - at least on the night side - and only the value of E_o used in (24) and (25) is changed. Note that the variation of R derived from (24) implies a time-dependent profile line, which might cause the trapping of particles initially on open trajectories.

Two final points may be worth pointing out. First, it should be noted again that the basic reason protons have more complex trajectories and can reach points near earth more easily than electrons of the same magnetic moment is that their co-rotation drift opposes their magnetic drift. If the earth's magnetic axis were reversed, these properties would hold for electrons rather than for protons.

Now from Pioneer 10 observations it appears that the magnetic dipole axis of Jupiter indeed is aligned in the opposite way from that of the earth, relative to the rotation vector. Observations made by that space-craft also indicate that Jupiter's magnetic field contains a very sizable ring current - causing distortions of the field comparable to those found in the earth's magnetic tail - and that in the trapped radiation found there, electrons greatly predominate (by contrast, the terrestrial ring current is mainly due to protons). This suggests that Jupiter might have an electric field similar to the earth's and that the same processes described here for protons are responsible for Jupiter's trapped electrons.

The second point is an analogy between the method of the profile line and the Clemmow-Mullaly-Allis (CMA) diagram for the propagation of waves in a cold two-component plasma [Stix, 1962] . In that case, the propagation of waves in any given plasma depends on an appropriate dispersion relation and there exists an infinity of such relations, depending on the magnetic field intensity B and on the plasma density n . If, however, one merely asks which propagation modes are possible in a given plasma, one only needs to know under what conditions modes appear or disappear. In the plane in which the cartesian coordinates are B and n (or suitable functions thereof) these conditions generally occur along certain lines, and a glance at the diagram in which all such lines are drawn, dividing the plane among various modes - which is the CMA diagram - quickly yields a large amount of useful qualitative information. In this analogy, Figure (4) corresponds to the CMA diagram, while contoured planes like those shown in Figures 1 - 3 , in which lines of constant W are mapped, correspond to graphs of the dispersion relation.

References

Chen, A.J., Penetration of Low Energy Protons Deep into the Magnetosphere, J. Geophys. Research 75, 2458-2467, 1970 .

Heppner, J.P., Electric Field Variations During Substorms: OGO-6 Measurements, Planet.Space Sci. 20, 1475-1498, 1972 .

McIlwain, C.E., Plasma Convection in the Vicinity of the Geosynchronous Orbit, in Earth's Magnetospheric Processes, B.M.McCormac Ed. , D. Reidel 1972, p. 268-279

Smith, P.H. and Hoffman, R.A., Ring Current Particle Distributions during the Magnetic Storms of December 16-18, 1971, J. Geophys. Res. 78, 4731-4737, 1973a.

Smith, P.H. and Hoffman, R.A., Quasi-Steady State Energy Spectrum for Ring Current Protons, (abstract) EOS (Transactions, AGU) 54, 1183 1973b .

Smith, P.H. and R.A. Hoffman (to be published, 1974)

Stern, D.P., Models of the Earth's Electric Field Goddard Space Flight Center Document X-602-74-159, May 1974.

Stix, T.H., The Theory of Plasma Waves, , McGraw Hill 1962 .

Captions to Figures and Table

Figure 1 Schematic structure of contours of constant W in the equatorial plane, for values of M for which $W_1 > W_3$ ($M < 0.04042$) . Below the contours the variation of W along the dawn-dusk line is schematically shown.

Figure 2 Similar to Figure 1 , for the range $0.04042 > M > M_o$ for which $W_1 < W_3$

Figure 3 Similar to Figure 1, for $M > M_o$, the regime in which the W_1 contour no longer exists.

Figure 4 The contours of $W_1(M)$, $W_2(M)$ and $W_3(M)$ in the (W,M) plane.

Figure 5 The relation between M and R along the line $W = W_1(M)$.

Figure 6 Similar to Figure 4 , with the profile lines drawn for $\rho = 5$, $\sin\varphi = 0, \pm 1$.

Table 1 Values of M corresponding to various values of R along the line $W = W_1(M)$. The plot of this relation is given in Figure 5 .

Table 1

R	M x 100	R	M x 100
0.585	6.840	0.73	3.943
0.6	6.816	0.74	3.460
0.62	6.706	0.75	2.930
0.64	6.495	0.76	2.350
0.66	6.171	0.77	1.718
0.68	5.720	0.78	1.032
0.7	5.129	0.79	0.290
0.72	4.381		

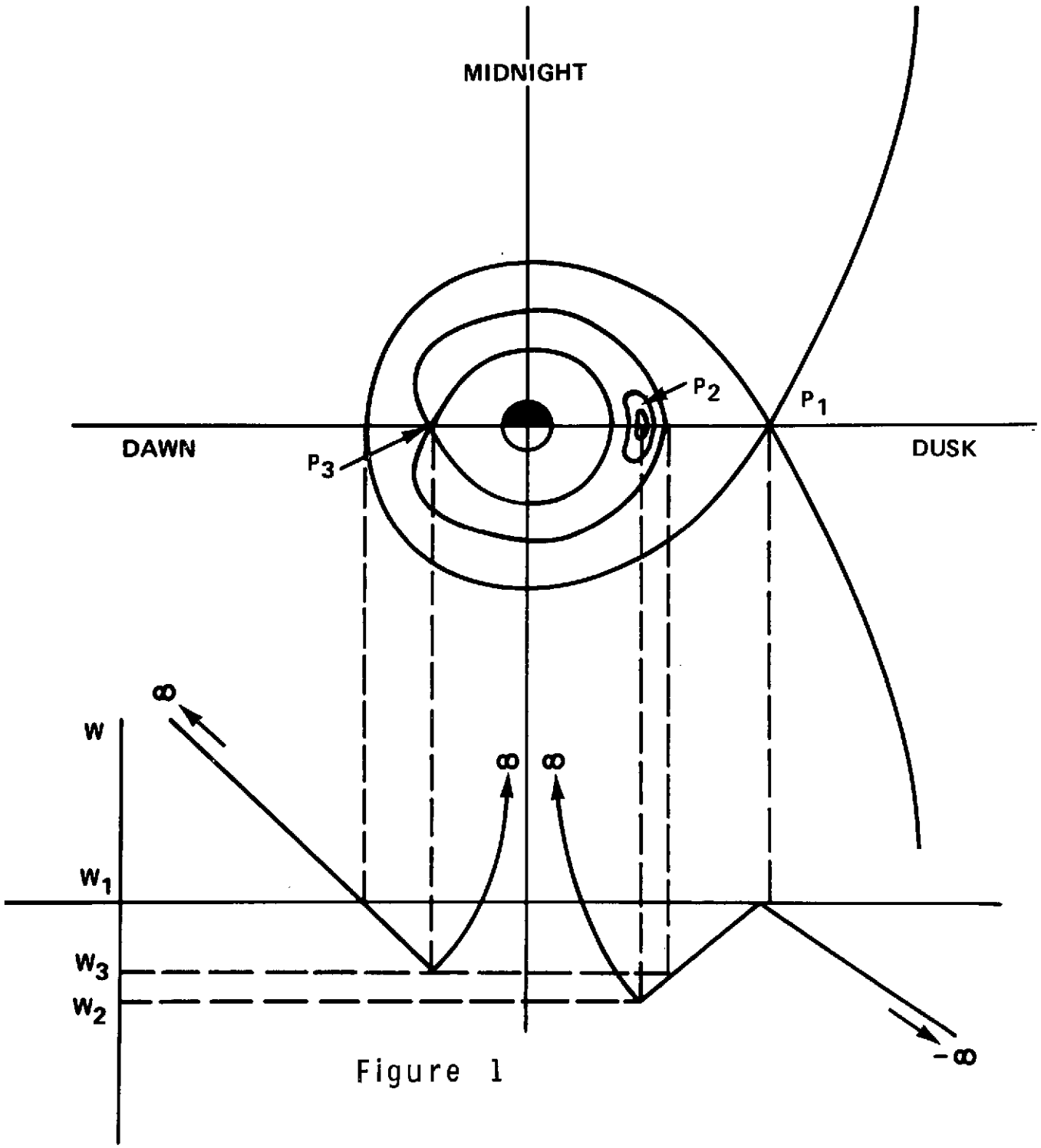

Figure 1

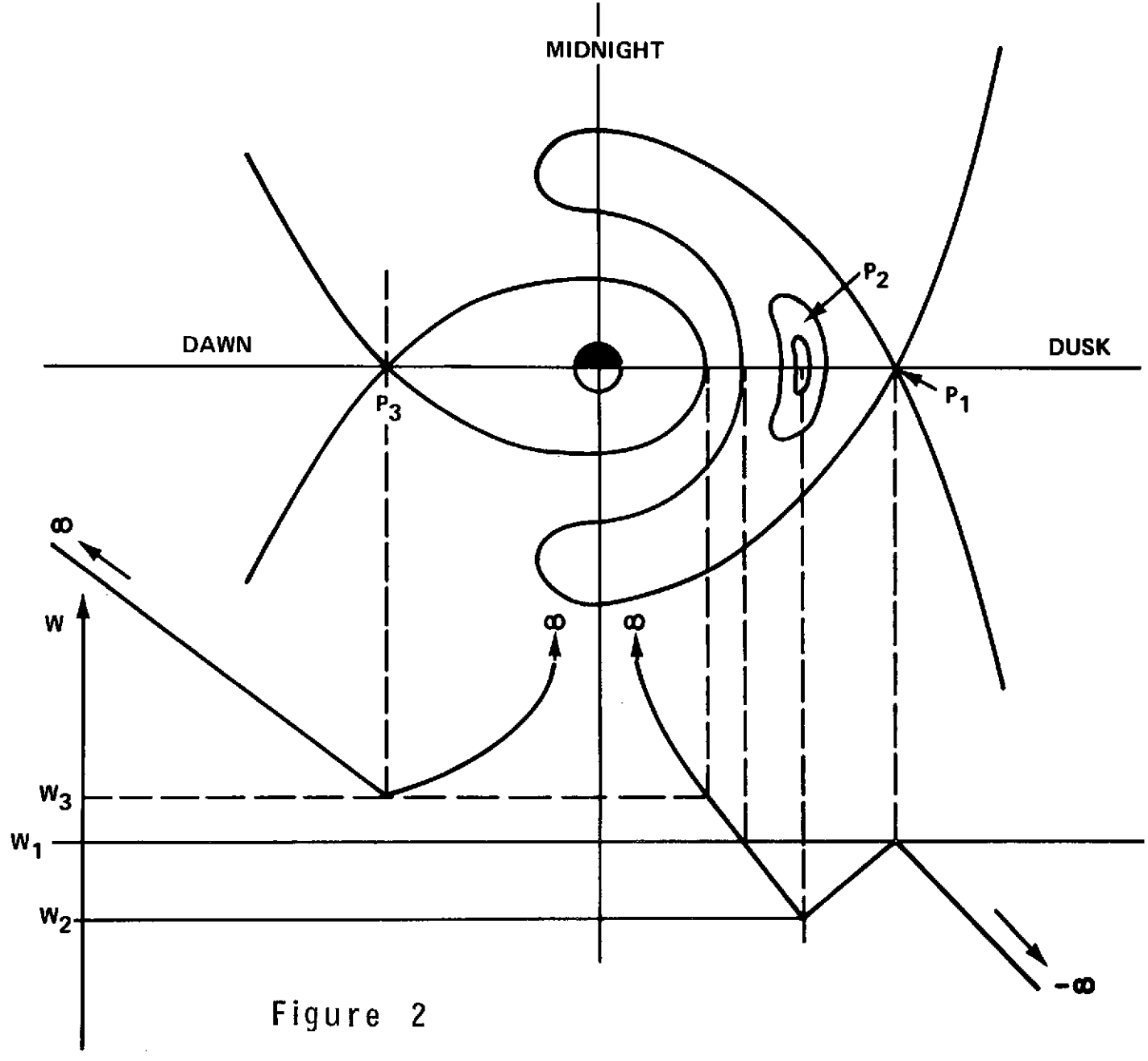

Figure 2

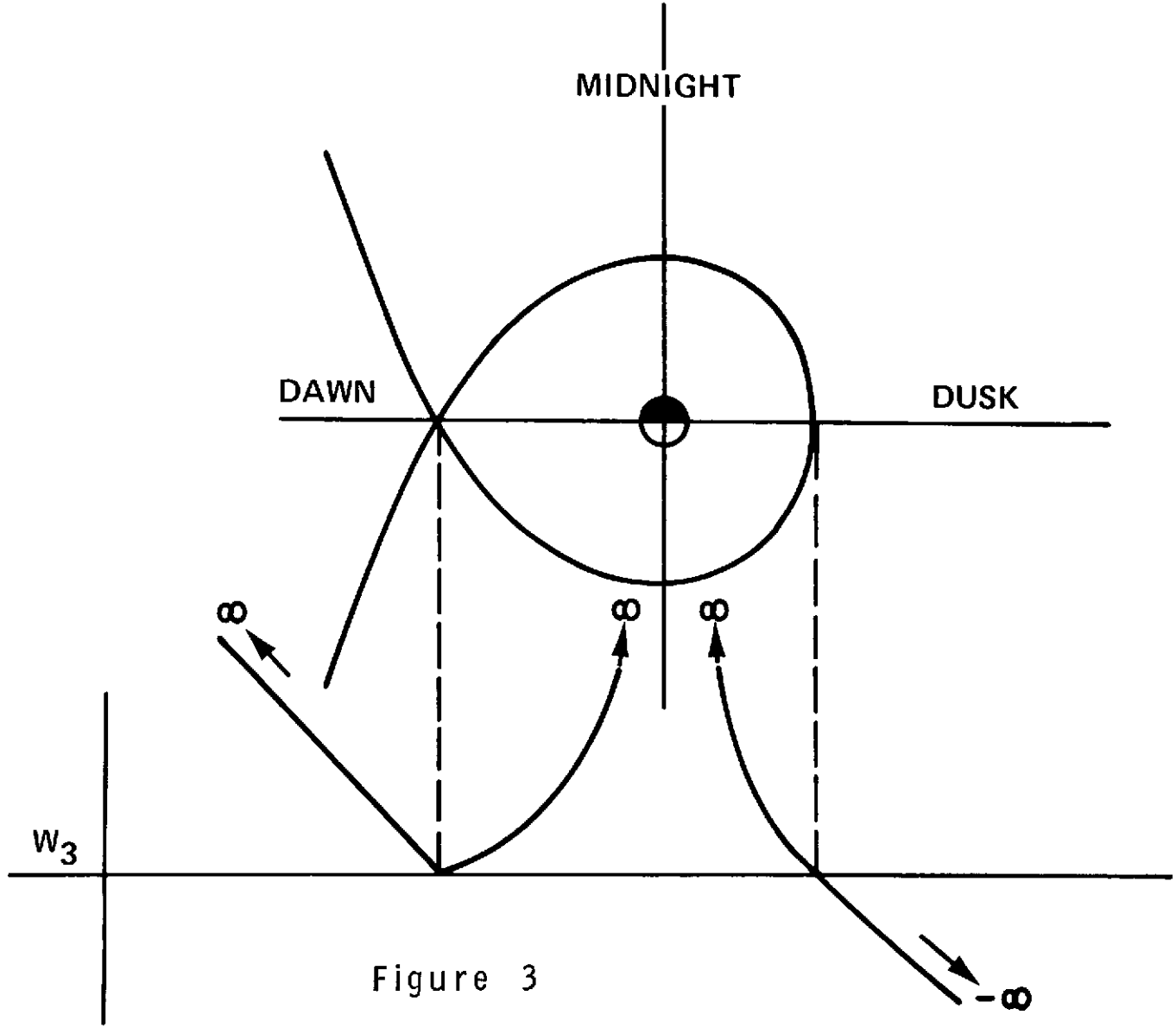

Figure 3

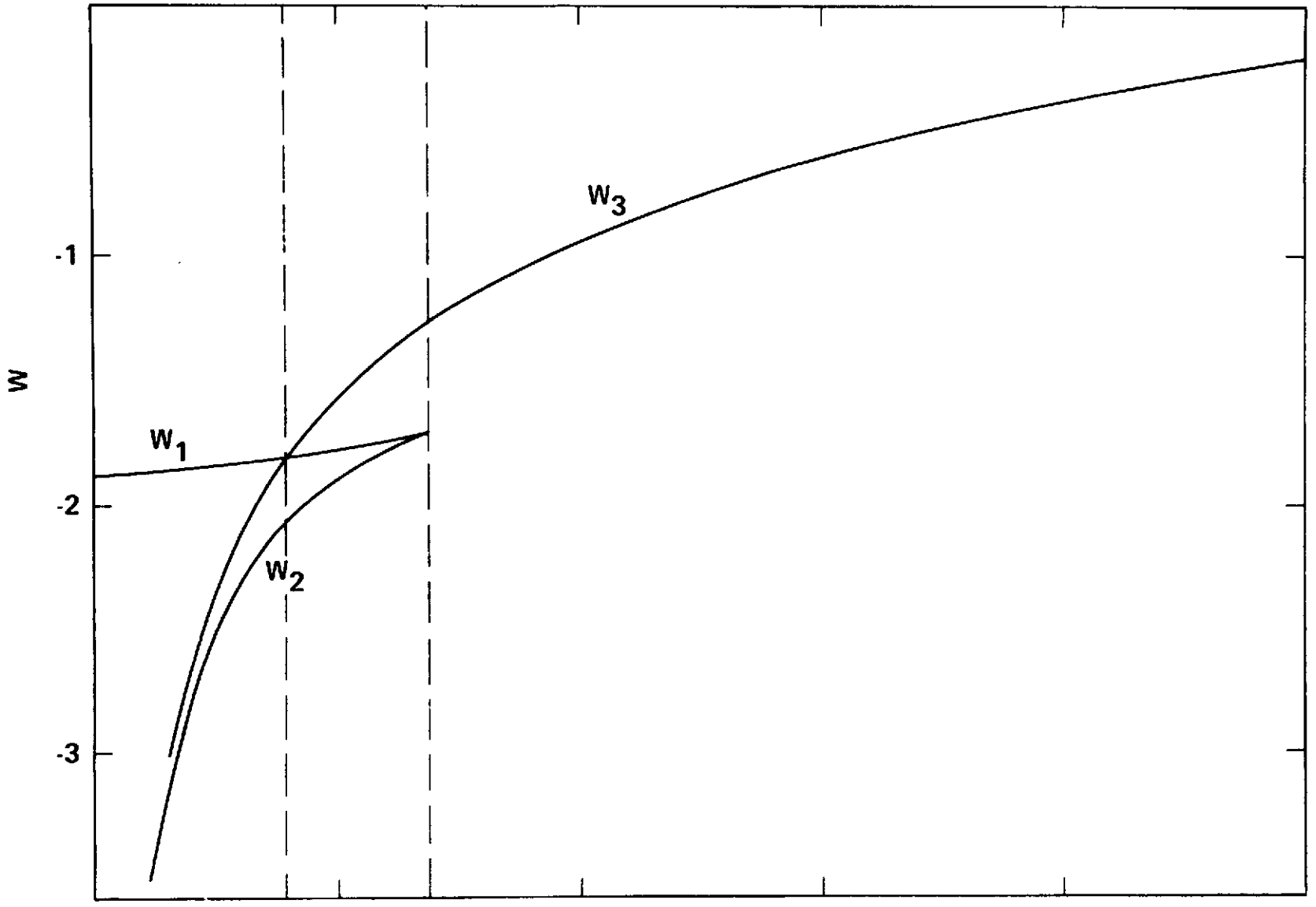

Figure 4

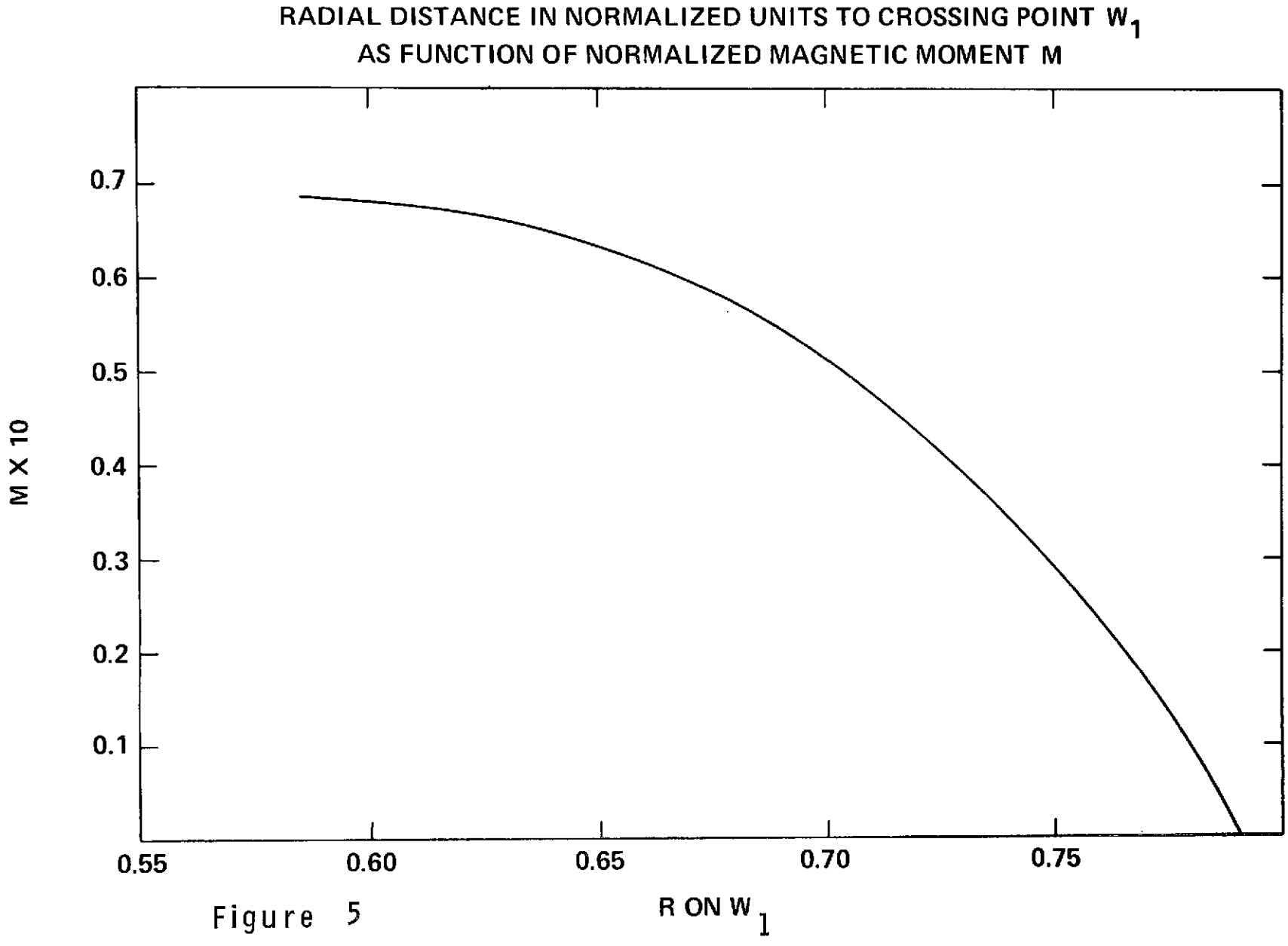
RADIAL DISTANCE IN NORMALIZED UNITS TO CROSSING POINT W_1
AS FUNCTION OF NORMALIZED MAGNETIC MOMENT M
M X 10
0.7
0.6
0.5
0.4
0.3
0.2
0.1
0.55
0.60
0.65
0.70
0.75
R ON W_1

Figure 5

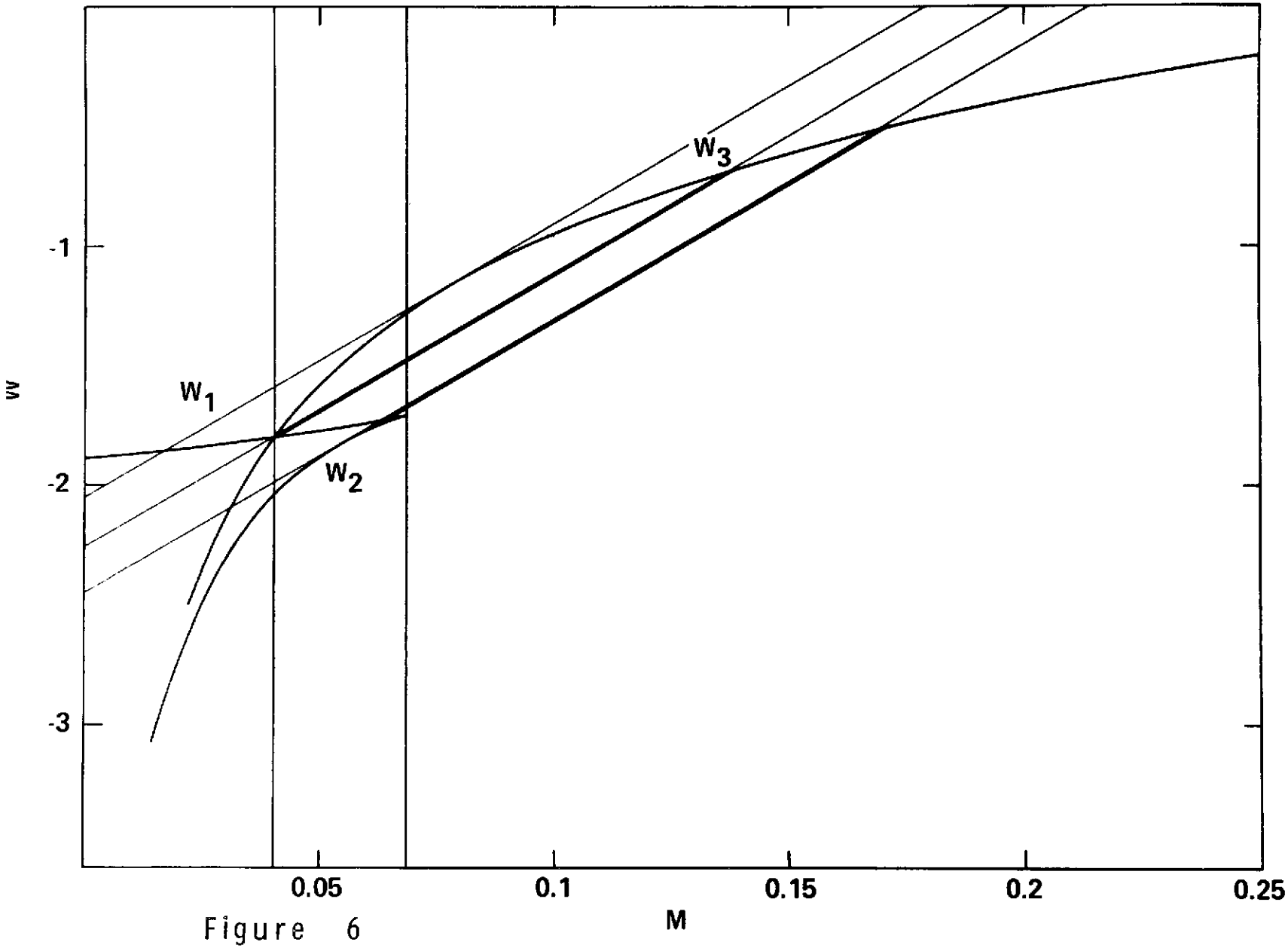

Figure 6

NASA–GSFC